CHIC – Coupling Habitability, Interior and Crust

A new Code for Modeling the Thermal Evolution of Planets and Moons

Lena Noack, Attilio Rivoldini, Tim Van Hoolst
Department of Reference Systems and Planetology
Royal Observatory of Belgium (ROB)
Brussels, Belgium
email: lena.noack@oma.be, attilio.rivoldini@oma.be, tim.vanhoolst@oma.be

***Abstract*—We present a new numerical code CHIC (*Coupling Habitability, Interior and Crust*) for the simulation of the thermal evolution of terrestrial planets, with a focus on the numerical aspects of the code and its validation. The thermal evolution of the mantle is calculated either by solving the energy conservation equation supplemented by boundary-layer theory (1D parameterized thermal evolution model) or by solving the energy, mass, and momentum conservation equations (2D/3D convective thermal evolution). For the latter setting, the equations can be solved either in the Boussinesq or extended Boussinesq approximation. The code provides information on the temperature field, convective velocities and convective stresses in the mantle. Simulations can also be run in steady-state regime. The code provides a user updatable library of thermodynamic properties of iron and common mantle silicates as well as associated equations of state, which allow to compute material properties at high pressure and temperature. CHIC has been benchmarked with different convection codes, and compared to published interior-structure models and 1D parameterized models. The CHIC code handles surface volcanism, crustal development, and different regimes of surface mobilization like plate tectonics. It is therefore well suited for studying scenarios related to the habitability of terrestrial planets. CHIC is an advanced simulation code that can be applied to a diverse range of geodynamic problems and questions.**

Keywords - fluid dynamics; convection; numerical modeling; thermal evolution; planetology.

I. INTRODUCTION

Numerical and parameterized models for convection and thermal evolution are essential tools to understand different geophysical processes in and between the interior of a planet and its atmosphere. These processes include for example the CO_2-cycle, the subduction cycle (delivering volatiles to the mantle), the release of volatiles by volcanic outgassing, the evolution of continents (stabilizing plate tectonics) and the possible maintenance of a magnetic field by strong cooling of the core. All those mechanisms may be important for the habitability of Earth, i.e., for its ability to host life, and may also play an important role for other planets. The magnetic field shields lighter volatiles in the atmosphere from erosion to space, whereas subduction of carbonates is an important phenomena that helps to regulate surface temperatures over geophysical timescales [1].

Several 2D and 3D convection codes have been developed over the past decades to investigate Earth-like planets. They typically concentrate solely on either the thermal evolution or do steady-state snapshots of the mantle and crust. Some models include the evolution of the core [2] or of the atmosphere [3][4]. Here, we describe a new code called CHIC that has been developed at the Royal Observatory of Belgium. The code is written in Fortran and is used to investigate different geophysical processes and feedback cycles on Earth-like planets. The planets are assumed to consist of several different spherical layers (shells). The lowermost shell represents the core and is overlain by a silicate shell (mantle and crust) and a potential water-ice layer. The uppermost shell represents the planet's atmosphere. All shells are thermally coupled, i.e., the heat flux and temperature are continuous at each interface between the different layers. The surface temperature is allowed to vary with time depending on the greenhouse gases in the atmosphere, or is taken constant if changes in the atmosphere are neglected.

The CHIC code is able to treat both 1D parameterized models (using the thermal boundary layer theory to determine the temperature evolution in a terrestrial or ocean planet) and 2D/3D models to investigate the detailed convection pattern in a silicate mantle or ice layer over time – both models have their advantages and disadvantages.

In a convection model (either modelling a 3D sphere or a 2D spherical annulus), lateral variations in the mantle can be investigated, including mantle plumes, local melt regions, and plate motions. A 1D model on the other hand assumes a laterally averaged profile for temperature and material properties like the density. As a result, simulations of, for example, the volcanic history of a terrestrial planet may differ between 1D and 2D/3D models.

1D thermal evolution models also have several advantages over 2D/3D convection models. The employed parameterization [5] is applicable to a large parameter space, including the simulation of both liquid and solid materials. Especially strongly convecting systems (e.g., liquid core or ocean) can be treated – which is generally unfeasible for planetary convection codes, as they will either produce numerical instabilities or require a high amount of computational power. 1D models, on the other hand, are very fast compared to convection models. Depending on the specific application, a 1D thermal evolution model runs in

 ISBN: 978-1-61208-416-9

the order of seconds or minutes, whereas 2D/3D models (that typically need a high resolution to avoid numerical errors) run for days or months.

CHIC couples a 1D parameterized module with a convection module in either 2D or 3D. The different modules can be applied as needed: for the core, either only changes in the core-mantle boundary (CMB) temperature are investigated, or a 1D model of the iron core including inner core freezing is applied (Figures 1(a) and 1(b)); the thermal state of the mantle and high-pressure ice layers are investigated either via a convection model or a 1D parameterized model; the atmosphere and a potential water ocean (Figures 1(c) and 1(d)) are investigated with a 1D module. CHIC is therefore a powerful tool for the investigation of the evolution of terrestrial or ocean planets - from interior to atmosphere - and their possible habitability.

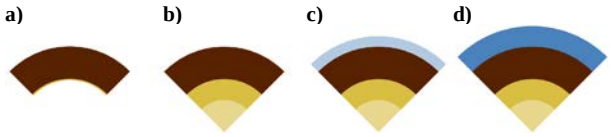

Figure 1. Possible configurations that are investigated with CHIC: a) mantle with variable CMB temperature, b) mantle with core evolution and inner core freezing, c) mantle and core with an atmosphere, d) mantle and core with a deep ocean on top (we neglect here a possible atmosphere).

The outline of the paper is as follows. In Section II, we describe the different modules of CHIC, followed by the benchmark results in Section III to show the validity of the code in various applications. Finally, in Section IV, we summarize the possibilities of a coupled 1D - 2D/3D code and the planned future work.

II. MODEL

CHIC uses various modules for the different shells of a terrestrial or ocean planet. The basic modules used in CHIC are listed below. The density of the material and other physical properties are determined as described in Section II-A, and can be applied to both 1D and 2D/3D modules. The input file used for the simulations is similar for all modules, which simplifies comparison of the 1D model with the 2D mantle model.

A. Interior structure model and material properties

We developed an interior structure model to assess the radius of a terrestrial planet for given mass and composition, and to determine the depth-dependent pressure, density and other thermodynamic properties for an initial temperature profile. We assume, that the planet is differentiated into an iron core, a silicate mantle (containing olivine, perovskite and post-perovskite) and an ocean layer. We derive average mantle and core values for the thermodynamic properties (e.g., thermal conductivity) to be used in the thermal evolution models.

To obtain profiles for the depth-dependent pressure p and gravity g, we solve the Poisson equation (1) and the hydrostatic pressure equation (2). The density ρ, the thermal expansion coefficient α and the heat capacity c_p at local conditions are obtained from equations of states of the relevant materials [6][7].

The gravitational acceleration g(r) depends on the gravity value at the surface of the planet (calculated from its mass and planet radius), the radius r and the density profile $\rho(r)$. G is the gravitational constant.

$$dg/dr = 4\pi G\rho - 2g/r \quad (1)$$

The gravitational and differential pressure forces are assumed to satisfy hydrostatic equilibrium. The pressure p decreases with increasing radius depending on local gravity and density, yielding a pre-defined atmospheric pressure at the surface:

$$dp/dr = -g\,\rho \quad (2)$$

The mass m(r) below a sphere of radius r increases with increasing radial coordinate until the pre-defined planet's mass M is reached.

$$dm/dr = 4\pi r^2\rho \quad (3)$$

Our interior structure model solves (1) to (3) by integration from the center of the planet outwards (starting from zero gravity and mass in the interior), thus yielding the radius of a planet for given composition (in terms of water, silicate and iron mass fraction) and mass.

B. Core evolution model

Our 1D core evolution module determines the variation of upper core temperature with time via the energy conservation equation

$$\rho_c c_{p,c} V_c \varepsilon_c dT_c/dt = -q_c A_c \quad (4)$$

where the index "c" denotes core values, V_c is the core volume and A_c the core surface area, ε_c is a constant relating the average core temperature to the CMB core temperature, t is the time and q_c is the heat flux from the core into the mantle

$$q_c = -k_m dT/dr|_{r=Rc} \quad (5)$$

We neglect radioactive heat sources in the core, as well as potential tidal heating effects. For 2D/3D convection models, the temperature gradient at the core-mantle boundary (CMB) is calculated over the two bottom shells of the mantle grid with laterally averaged temperatures; in the 1D parameterized model, the temperature drop over the lower thermal boundary layer of the mantle is used instead.

We either treat the core consisting of pure iron or a mixture of iron and lighter elements like sulfur. We can consider possible freezing of the core, when the core temperature falls below the melting temperature. This model, however, only works if the freezing of the core starts at the

 ISBN: 978-1-61208-416-9

core center (leading to a solid inner core as on Earth). This may not be the case for Mercury or Ganymede, where iron may solidify in the upper part of the core and sink down as (so-called) iron snow. We only model planets without the iron snow regime and adopt the model of [2], which determines latent heat released by iron solidification and gravitational energy produced by differentiation of the core into an inner and outer core. Both mechanisms lead to an increasing temperature at the CMB temperature and thus have an influence on the thermal evolution of the mantle, as well. For super-Earths (i.e., planets up to 10 Earth masses), we neglect lighter elements in the core, as the EOS for mixtures of iron and lighter elements have only been derived in a limited pressure range not suitable for super-Earths.

C. Mantle: 1D parameterized model

The 1D module to assess the thermal evolution of the mantle of a terrestrial planet is based on [5][8]. We refer to these references for full details on the model. The model determines the evolution of the upper mantle temperature T_m over time by considering that the loss of energy due to mantle cooling and heat flux out of the mantle is balanced by the heat flux into the mantle and the radioactive heat production in the mantle:

$$\rho_m c_{p,m} V_l \varepsilon_m dT_m/dt = -q_l A_l + q_c A_c + Q_m V_l \qquad (6)$$

The index "m" denotes mantle values. V_l is the volume of the mantle from core to lithosphere (thus excluding the conductive lithosphere), and A_l is the area at the boundary between mantle and lithosphere. The constant ε_m relates the average mantle temperature and T_m. The mantle temperature decreases due to heat flux out of the mantle into the lithosphere q_l, increases due to inflowing heat flux from the core q_c and increases with heat released by radioactive heat sources Q_m.

We also consider possible melting events and crust formation over time, leading to additional terms in (6). For details on the crustal evolution, as well as the definition of the thermal boundary layers and calculation of the temperature in the lithosphere, we refer to [8].

Note, that the 1D parameterized model only considers the evolution of the temperature over time, and assumes effective convection. To understand the convection mechanism and its strength depending on mantle parameters and planet size (possibly triggering plate tectonics at the surface), a more sophisticated 2D/3D convection model is needed.

D. Mantle: 2D / 3D convection model

The CHIC code uses a finite volume (FV) field approach to solve the conservation equations of mass, momentum and energy. A finite grid is placed in the mantle, with shells from the CMB to the planet surface, and a predefined number of grid points per shell. We then define Voronoi cell volumes around each grid point and solve the system of equations on each cell volume considering the flux in and out of the cell and the energy production in the cell, see Figure 2.

The grid is either defined in Cartesian coordinates in a 2D or 3D box or in polar coordinates for a 2D cylindrical sphere (a cut through the planet at the equator representing the temperature profile of a cylinder with the 2D plane as a basis) or a 2D spherical annulus (an equatorial cut that mimics the temperature profile of a sphere in 3D, [9]). For the 2D models with spherical or cylindrical geometry, it is often useful to employ a regional sector of the 2D spherical model (as shown in Figure 4) to save computational power. In addition to the grid, randomly distributed particles, that move along the convective stream lines, are used to transport local information as for example the water content.

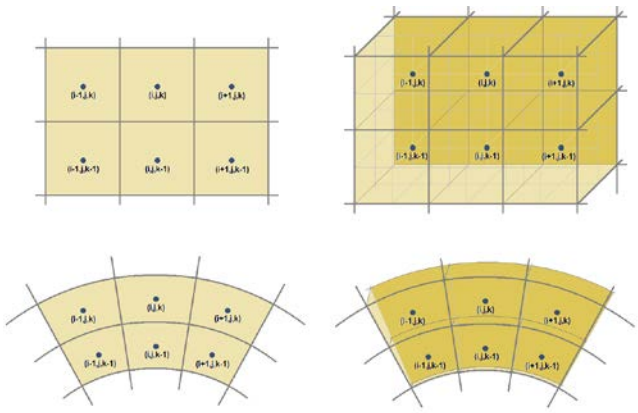

Figure 2. Geometries implemented in CHIC. Top: 2D Cartesian box and 3D Cartesian box. Bottom: 2D cylinder and 2D spherical annulus.

We solve the equation system for an incompressible medium with the Extended-Boussinesq approximation (EBA), which yields an adiabatic temperature increase with depth (see [5] for details on the model). For a dissipation number Di of zero, the formulation reduces to the Boussinesq approximation (BA).

In the EBA approximation, the non-dimensional conservation equations of energy, mass and momentum can be expressed as [10]

$$\partial T/\partial t + u \cdot \nabla T + Di(T+T_0)u_r = \nabla^2 T + 0.5 Di\, \eta \dot{\varepsilon}_{II}^2/Ra + H \qquad (7)$$

$$\nabla \cdot u = 0 \qquad (8)$$

$$\nabla P - \nabla[\eta(\nabla u + \nabla u^T)] = Ra\, T\, e_r \qquad (9)$$

Here, T is temperature, T_0 surface temperature, t time, and Di the dissipation number. The convective pressure is denoted by P; u is the velocity and u_r the radial velocity, whereas e_r is the radial unit vector. The Rayleigh number Ra is a measure for the convective vigor of the material, and H is the heat source (e.g., radioactive heat source). η is the viscosity and $\dot{\varepsilon}_{II}$ is the second invariant of the strain rate.

The equations (7)-(9) are written in a non-dimensional form, as is typically done for convection simulations [11]. The non-dimensionalization is obtained by dividing the dimensional value of each variable by a reference value as

 ISBN: 978-1-61208-416-9

given in [11]. The quantities given in Section III are also non-dimensional values.

The energy equation is solved with a second-order implicit Euler method. For the results reported here, we also apply an upwind scheme. To solve the conservation equation of mass and momentum, we either use a direct solver or a coupled mass and momentum solver. The direct solver uses one solver matrix for (8) and (9) and applies a penalty formulation following [12]. The iterative, coupled solver employs a SIMPLER pressure correction algorithm following [12][13]. In this paper, we apply the direct solver.

The resulting linear equations (for mass, momentum and energy equation) are solved iteratively using either the Fortran Pardiso solver [14] or a biconjugate gradient (BiCG) solver with an under-relaxation scheme. The BiCG solver is slower compared to the Pardiso solver but can be easily parallelized.

The equations above depend on the viscosity of the material η. The viscosity depends on several factors including the temperature, pressure, grain size, water content and strain rate of a material. In Earth's mantle, creep of minerals is typically described by dislocation creep (motion of dislocations through the crystal lattice) and diffusion creep (deformation of crystalline solids by the diffusion of vacancies through their crystal lattice). The latter is largely independent of the strain-rate, whereas dislocation creep does not depend on the grain size. In CHIC, the user can choose between a dislocation viscosity, a diffusion viscosity and a mix of both formulations. The smaller viscosity is the dominant viscosity for material motion.

The general equation that we use for the viscosity follows an Arrhenius law [15][16]

$$\eta = A\dot{\varepsilon}_{II}^{1-n/n} d^{p/n} C_{OH}^{-r/n} \exp(\,(E+pV)/(nRT)\,) \qquad (10)$$

A is a material-dependent constant, n is the stress exponent, d is the grain size, C_{OH} is the concentration of water (for dry materials r=0), r is the water exponent, E the activation energy and V the activation volume. p is the pressure and R the gas constant. Note, that the pressure p is the hydrostatic pressure and not the convective pressure as in (9). The parameters for both diffusion and dislocation creep are taken from [15][16] for both wet and dry materials. The concentration of water C_{OH} is traced via particles in CHIC and does not only influence the viscosity, but also the local melt temperature, which is smaller in the presence of water than for dry materials [17].

Note, that even though the Arrhenius viscosity (10) is preferentially used for simulations of terrestrial planets, for benchmarks and basic convection simulations, often an approximated viscosity is used, the so-called Frank-Kamenetskii approximation (FKA), given by

$$\eta = A \exp(-\gamma_T T + \gamma_p z) \qquad (11)$$

Here, γ_T and γ_p are either the logarithm of a pre-defined viscosity contrast with respect to temperature or pressure, respectively, or they are derived from the parameters in (10) [18]. z is the non-dimensional depth (0 at the surface and 1 at the CMB). Note, that for the application to terrestrial planets (especially for plate tectonics planets), the FKA (11) is not suitable and the Arrhenius viscosity (10) should be applied [18].

E. Additional modules

CHIC can also be used for ocean planets and icy moons, where a silicate-iron shell is covered by a deep water or ice sphere. Another module treats the evolution of the atmosphere with time, where we consider outgassing of greenhouse gases CO_2 and H_2O. The model can be applied to planets with a Mars- or Venus-like atmosphere [3].

III. RESULTS AND DISCUSSION

To validate our code, we applied several benchmark tests for the convection module. To our knowledge, unlike for the mantle convection calculation, benchmark results for the 1D parameterized model have not been published. Therefore, we have validated our code by reproducing results of [8]. The results are very similar [19], but differ in detail because not all parameters used in the studies are known. The module has been integrated into the CHIC code and has been extended to include a regolith layer and compared to [20], yielding again comparable results.

We compared our 1D parameterized model to the convection module by applying the 2D spherical annulus. In Figure 3, we plot the thermal evolution of Mars determined for a Boussinesq approximation, a Newtonian viscosity law (n=1 in (10)) and fit the pre-factor such that we obtain a reference viscosity of 10^{20} Pas at 1600 K and 3 GPa. We use an activation energy of E=300 kJ/mol and an activation volume of 2.5 cm^3/mol. The initial mantle temperature is 2000 K and the CMB temperature is 2300 K, the surface temperature is set to 220 K. Heat sources are homogeneously distributed in the mantle and are taken Earth-like [5]. For the 2D model, we use a quarter sphere with a radial resolution of 80 shells.

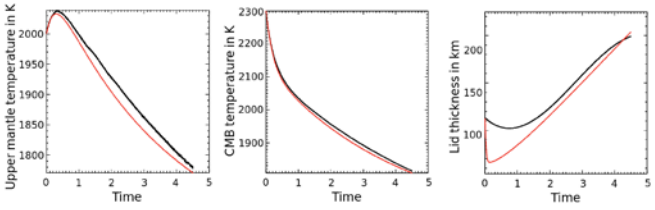

Figure 3. Upper temperature, CMB temperature and lid thickness for a thermal evolution of Mars applying either the 2D spherical annulus (black curve) or the 1D parameterized model (red).

The mantle initially heats up due to radioactive decay, convection then leads to efficient cooling of the mantle. In the convection model, we define the lid over the depth where the conductive heat transport is more efficient than the convective heat transport. The lid thickness is then fitted by a third-order polynomial since oscillations occur. The obtained lid thickness is in the beginning larger than for the 1D model

 ISBN: 978-1-61208-416-9

(where we plot the total conductive layer thickness including both the lid and the upper thermal boundary layer), but shows a similar increase with time after 2Gyr. The different lid thicknesses at the beginning of the evolution can be explained by a delayed on-set of convection in the 2D model, which also leads to a slightly weaker mantle cooling at the beginning and hence a shift in the upper mantle temperature compared to the 1D model.

For the convection model, we applied several standard benchmarks published in the literature. The most basic benchmark has been developed for convection in a 2D Cartesian box [21] and uses either isoviscous convection or temperature- and pressure-dependent viscosity in the Boussinesq approximation. A free-slip boundary condition is applied to the walls of the box. The non-dimensional temperature at the surface of the box is set to 0 and at the bottom to 1. The simulations are run until steady-state is reached (i.e., temperature variations drop below a tolerance value of 10^{-10}).

In Table I, we compare our results (for a fixed resolution of 80(200)x80 cells, depending on the aspect ratio) to published results. Note, that in [21] different resolutions have been used, and we give the min and max values for resolutions of at least 33x33 cells. We list the three most important quantities: the root-mean-square (RMS) velocity, the maximum of the upper mantle temperature profile at the middle (x=0.5ℓ, where ℓ is the length divided by height, i.e., the aspect ratio) and the surface Nusselt number, which is a measure of the ratio of convective to conductive heat transport at the surface of the box. For more information on the benchmark setup we refer the reader to [21]. CHIC yields results in good agreement with all cases published in [21], see Table I, and lies either in the range of published results or differs by less than 0.5%.

TABLE I. BENCHMARK COMPARISON OF CHIC (CH) TO [21] (BL).

	RMS velocity		*Max temperature*		*Nusselt number*	
	CH	**BL**	**CH**	**BL**	**CH**	**BL**
1a	42.92	42.74-42.87	0.425	0.421-0.427	4.920	4.864-4.896
1b	194.3	192.4-198.0	0.432	0.415-0.437	10.60	10.42-10.69
1c	835.1	823.7-842.5	0.440	0.431-0.446	21.81	21.08-22.07
2a	496.6	458.3-503.3	0.725	0.716-0.741	10.43	10.04-10.07
2b	183.1	166.7-193.1	0.390	0.385-0.403	7.271	6.806-7.409

C1: isoviscous material, ℓ=1, a) Ra=1e4, b) Ra=1e5, c) Ra=1e6.
C2: FKA (11), a) Ra_{surf}=1e4, γ_T=ln(1000), γ_p=0, ℓ=1, b) Ra_{surf}=1e4, γ_T=ln(16384), γ_p=ln(64), ℓ=2.5.

A similar benchmark has been published in [10] for the Extended Boussinesq approximation and compressible materials in a 2D Cartesian box. We compare the benchmark results using EBA (see Section IID) for a resolution of 80x80 cells to the results in [10], see Table II.

CHIC compares well to the published results for EBA with deviations of few percent at most. A similar benchmark for a 2D cylindrical shell including compressibility is in preparation for publication and includes 10 different codes, including CHIC. The accuracy of the CHIC code is comparable to the Cartesian simulations.

TABLE II. BENCHMARK COMPARISON OF CHIC (CH) TO [10] (KI).

	RMS velocity		*Average temperature*		*Nusselt number*	
	CH	**KI**	**CH**	**KI**	**CH**	**KI**
1a	38.38	38.39-38.50	0.4911	0.4909-0.4914	4.125	4.05-4.10
1b	61.43	61.35-61.50	0.4935	0.4937-0.4942	5.203	5.10-5.16
1c	111.7	111.5-111.7	0.4980	0.4987-0.4996	6.997	6.86-6.95
1d	174.0	173.5-174.2	0.5018	0.5033-0.5045	8.710	8.54-8.66
1e	269.2	267.9-269.5	0.5056	0.5083-0.5101	10.80	10.6-10.7
1f	474.2	465.0-466.8	0.5097	0.5161-0.5178	14.25	13.9-14.1
2a	33.70	33.76-33.92	0.4822	0.4816-0.4823	3.408	3.34-3.38
2b	54.14	54.17-54.41	0.4854	0.4851-0.4861	4.255	4.16-4.22
2c	98.36	98.80-98.86	0.4920	0.4926-0.4940	5.648	5.52-5.60
2d	152.3	152.3-153.4	0.4980	0.4997-0.5017	6.957	6.79-6.90
2e	232.8	231.0-232.8	0.5041	0.5080-0.5109	8.516	8.26-8.40
3a	23.78	23.95-24.24	0.4678	0.4658-0.4671	2.209	2.15-2.19
3b	38.77	39.07-39.50	0.4685	0.4664-0.4682	2.675	2.60-2.65
3c	70.22	70.85-71.66	0.4734	0.4719-0.4747	3.399	3.30-3.36
3d	106.4	107.1-108.2	0.4793	0.4789-0.4823	4.031	3.89-3.97
3e	152.3	147.0-148.0	0.4868	0.4893-0.4938	4.663	4.40-4.44

C1: Di=0.25, ℓ=1, a) Ra=1e4, b) Ra=2e4, c) Ra=5e4, d) Ra=1e5, e) Ra=2e5, f) Ra=5e5.
C2: Di=0.5, ℓ=1, a) Ra=1e4, b) Ra=2e4, c) Ra=5e4, d) Ra=1e5, e) Ra=2e5.
C3: Di=1.0, ℓ=1, a) Ra=1e4, b) Ra=2e4, c) Ra=5e4, d) Ra=1e5, e) Ra=2e5.

A two-code benchmark for the different geometries (between CHIC and GAIA [22]) has been realized for a Boussinesq material [23]. For the 2D box, we apply a resolution of 80(160 for ℓ=2)x80 cells, for the 3D box 20x20x20 cells and for the 2D shells we apply 80 shells in radial direction with 754, 377, 189, 440, 419 and 754 points per shell for the 6 considered cylindrical/spherical cases. Note, that we compare the 2D spherical annulus of CHIC to the case of 3D sphere of GAIA.

Both codes are well in agreement, with deviations below 5% apart from the 3D box (12.5% deviation), where we applied a lower resolution than in [23], see Table III. The plots in Figure 4 show the steady-state for all cases.

TABLE III. BENCHMARK COMPARISON OF CHIC (CH) TO [23] (NT).

Case	*RMS velocity*		*Average temperature*		*Top Nusselt number*	
	CH	**NT**	**CH**	**NT**	**CH**	**NT**
2D box, ℓ=1, RBC [a]	55.73	53.06	0.6904	0.6872	2.001	1.956
2D box, ℓ=2, RBC [a]	55.73	53.79	0.6904	0.6871	2.001	1.956
2D box, ℓ=1, PBC [b]	56.88	54.62	0.7038	0.6993	2.069	2.014
3D box, ℓ=1, RBC	65.43	57.21	0.6997	0.6927	2.200	2.363
2D full cylinder [c]	36.24	35.25	0.5744	0.5711	1.439	1.439
2D half cylinder	35.64	34.84	0.5751	0.5725	1.435	1.440
2D quarter cylinder	35.64	34.87	0.5751	0.5725	1.435	1.440
2D cylinder, CV [d]	16.80	17.11	0.4362	0.4377	0.967	0.995
2D cylinder, CR [e]	14.46	14.51	0.4046	0.4039	0.891	0.914
3D sphere [f]	15.56	16.19	0.3657	0.3374	0.782	0.744

We apply a surface Rayleigh number of Ra=10 and a FKA (11) viscosity contrast of 1e5.
[a] RBC stands for reflective boundary condition at the side wall with free-slip boundary.
[b] PBC stands for periodic boundary conditions.
[c] The sphere uses a radius ratio of 2, i.e., the core radius is half the planet radius.
[d] CV means corrected volume such that ratio of core area divided by mantle volume is as in 3D.
[e] CR means corrected radius such that ratio of core area divided by surface area is as in 3D.
[f] We use a 2D spherical annulus instead of a 3D sphere with 4 initial plumes instead of 6.

 ISBN: 978-1-61208-416-9

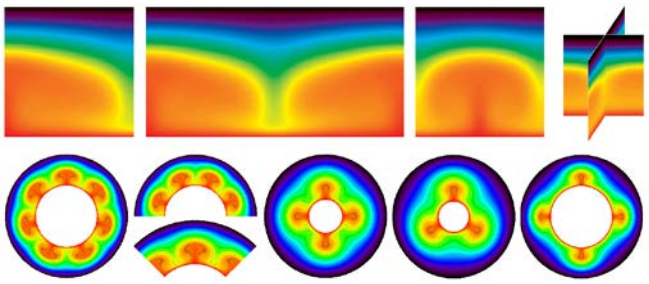

Figure 4. Convection patterns obtained with CHIC for different available geometries. See text and Table III for more details.

The 2D spherical annulus furthermore has been compared to the results in [9]. The non-dimensional radius of the core is 1.2222 and the planet radius is 2.2222. We use a resolution of 32 shells with 256 points on each shell. The CHIC results are well in agreement with the published steady-state results, with differences of not more than 6%, see Table IV.

TABLE IV. BENCHMARK COMPARISON OF CHIC (CH) TO [9] (HT).

	Ra	***Average RMS velocity***		***Nusselt number***	
		CH	**HT**	**CH**	**HT**
1	1e4	39.87	37.7	4.39	4.18
	1e5	174.1	~160	7.61	~7.39
	1e6	719.3	~640	16.53	~14.4
	Ra / H	***Average RMS velocity***		***Average mantle temperature***	
2	1e4 / 3.4	25.09	23.5	0.295	0.308
	1e5 / 6.6	~97	~78.5	~0.369	~0.349
	1e6 / 14	~340	~265	~0.385	~0.350

isoviscous material, case 1: bottom-heated convection, case 2: internally-heated convection.

For time-dependent simulations (indicated by "~"), larger deviations can appear between different codes (here up to 22%). For this reason typically only steady-state simulations are used in community benchmarks.

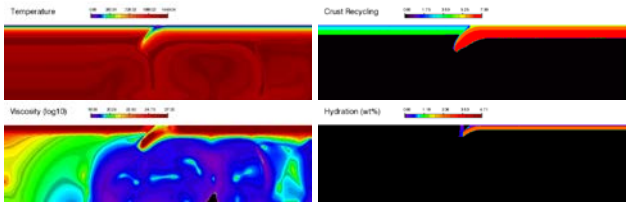

Figure 5. Simulation of the subduction process of an oceanic plate including dehydration of the subducted slab and related melting processes.

Recently, an increasing attention has been drawn to benchmarks for time-dependent simulations, for example for surface mobilization in a subduction zone (Figure 5, in preparation for publication), or for plastic deformation and episodic overturn [24].

IV. CONCLUSION AND FUTURE WORK

CHIC is a new, advanced numerical code developed at the Royal Observatory of Belgium, and can be applied to different geodynamic applications, including the simulation of the thermal evolution of terrestrial planets. Both 1D and 2D/3D geometries can be applied to the silicate mantle to investigate the thermal evolution (as well as convection and surface mobilization for the 2D models). The core, the ocean layer and the atmosphere are solved with the parameterized model. The thermal evolution of Mars' mantle has been investigated with both the 1D model and the 2D spherical annulus model with comparable results. Furthermore, the code has been validated by comparison to published 1D parameterized models and benchmarks for the 2D/3D mantle convection model for all available geometries (Figure 4). CHIC is in good agreement with literature values. New benchmark projects with contributions from CHIC are currently in preparation for publication or in review. Readers interested in access to the code are asked to directly contact the authors of the paper.

ACKNOWLEDGMENT

L. Noack has been funded by the Interuniversity Attraction Poles Programme initiated by the Belgian Science Policy Office through the Planet Topers alliance. A. Rivoldini was supported by the PRODEX program managed by the European Space Agency in collaboration with the Belgian Federal Science Policy Office. This work results within the collaboration of the COST Action TD 1308. We thank Clemens Heistracher, Nastasia Zimov, François Labbé, and Thomas Boiveau for their contributions to the project.

REFERENCES

[1] P. van Thienen et al., "Water, Life, and Planetary Geodynamical Evolution", Space Sci. Rev., vol. 129, 2007, pp. 167-203.

[2] G. Schubert, M. N. Ross, D. J. Stevenson, and T. Spohn, "Mercury's thermal history and the generation of its magnetic field", in Mercury, 1998, pp. 429-460.

[3] L. Noack, D. Breuer, and T. Spohn, "Coupling the atmosphere with interior dynamics: Implications for the resurfacing of Venus", Icarus, vol. 217, 2012, pp. 484-498.

[4] C. Gillmann and P. Tackley, "Atmosphere/mantle coupling and feedbacks on Venus", JGR Planets, vol. 119, 2014, pp. 1189-1217.

[5] G. Schubert, D. L. Turcotte, and P. Olson, "Mantle Convection in the Earth and Planets", Cambridge University Press, Cambridge, 2001.

[6] L. Stixrude and C. Lithgow-Bertelloni, "Thermodynamics of mantle minerals--I. Physical properties", GJI, vol. 162(2), 2005, pp. 610-632.

[7] J. Bouchet, S. Mazevet, G. Morard, F. Guyot, and R. Musella, "Ab initio equation of state of iron up to 1500 GPa", Physical Review B, vol. 87 - 094102, 2013, pp. 1-8.

[8] A. Morschhauser, M. Grott, and D. Breuer, "Crustal recycling, mantle dehydration, and the thermal evolution of Mars", Icarus, vol. 212(2), 2011, pp. 541-558.

[9] J. W. Hernlund and P. Tackley, "Modeling mantle convection in the spherical annulus", PEPI, vol. 171, 2008, pp. 48-54.

[10] S. D. King et al., "A community benchmark for 2D cartesian compressible convection in the Earth's mantle", GJI, vol. 180(1), 2010, pp. 73-87.

 ISBN: 978-1-61208-416-9

[11] U. R. Christensen, “Convection with pressure- and temperature-dependent non-Newtonian rheology”, Geophys. J. R. astr. Soc., vol. 77, 1984, pp. 343-384.

[12] S. Zhong, D. A. Yuen and L. N. Moresi, “Numerical methods in mantle convection”, Treatise on Geophysics, vol. 7, 2007, pp. 227-252.

[13] S. V. Patanker, “A calculation procedure for two-dimensional elliptic situations”. Numerical Heat Transfer V, 1981, pp. 409-425.

[14] O. Schenk and K. Gärtner, “On fast factorization pivoting methods for symmetric indefinite systems”, Elec. Trans. Numer. Anal., vol. 23, 2006, pp. 158-179.

[15] S.-i. Karato and P. Wu, “Rheology of the upper mantle: a synthesis”, Science, vol. 260, 1993, pp. 771-778.

[16] G. Hirth and D. Kohlstedt, “Rheology of the upper mantle and the mantle wedge: a view from the experimentalists”, in Eiler, J. (Ed.), Inside the Subduction Factory. Geophysical Monograph Series, vol. 138, AGU, Washington, D.C., 2003, pp. 83-105.

[17] R. Katz, M. Spiegelman, and C. Langmuir, “A new parameterization of hydrous mantle melting”, G^3, vol. 4(9) - 1073, 2003, pp. 1-19.

[18] L. Noack and D. Breuer, “First- and second-order Frank-Kamenetskii approximation applied to temperature-, pressure- and stress-dependent rheology”, GJI, vol. 195, 2013, pp. 27-46.

[19] T. Boiveau, “Convection mantellique dans les planètes telluriques”. Rapport de stage, unpublished.

[20] N. Tosi, M. Grott, A.-C. Plesa, and D. Breuer, “Thermochemical evolution of Mercury’s interior”, JGR Planets, vol. 118, 2013, pp. 1-14.

[21] B. Blankenbach et al., “A benchmark comparison for mantle convection codes”, GJI, vol. 98, 1989, pp. 23-38.

[22] C. Hüttig and K. Stemmer, ”Finite volume discretization for dynamic viscosities on Voronoi grids”, PEPI, vol. 171, 2008, pp. 137-146.

[23] L. Noack and N. Tosi, “High-performance modelling in geodynamics”, in Integrated Information and Computing Systems for Natural, Spatial, and Social Sciences, ed. Rückemann, C.-P., IGI Global, 2013, pp. 324-352.

[24] N. Tosi et al., “A community benchmark for viscoplastic thermal convection in a 2-D square box”, G^3, in review.

 ISBN: 978-1-61208-416-9